

ELECTRONIC SUPPORTING INFORMATION

1,2-Azolyamidino Ruthenium(II) Complexes with dmso Ligands: Electro- and Photocatalysts for CO₂ Reduction

Murphy Jennings,^a Elena Cuéllar,^b Ariadna Rojo,^b Sergio Ferrero,^b Gabriel García-Herbosa,^c John Nganga,^d
Alfredo M. Angeles-Boza,^{a,d} Jose M. Martín-Alvarez,^b Daniel Miguel,^b and Fernando Villafañe*^b

a) Institute of Materials Science, University of Connecticut, 97 N. Eagleville Rd, Storrs, CT 06269, USA.

b) GIR MIOMeT-IU Cinquima-Química Inorgánica, Facultad de Ciencias, Campus Miguel Delibes, Universidad de Valladolid, 47011 Valladolid, Spain. E-mail: fernando.villafane@uva.es

c) Departamento de Química, Facultad de Ciencias, Universidad de Burgos, 09001 Burgos, Spain.

d) Department of Chemistry, University of Connecticut, 55 N. Eagleville Rd, Storrs, CT 06269, USA.

Table of contents	
Table S1. Electrochemical data obtained by cyclic voltammetry in this study, in DMF	4
Figure S1. Cyclic voltammograms of all complexes	5
Figure S2. Cyclic voltammograms scan rates complex 1b	6
Figure S3. Cyclic voltammograms scan rates complex 2b	7
Figure S4. Cyclic voltammograms scan rates complex 3b	8
Figure S5. Cyclic voltammograms of 1b , 2b , 3b with proton source	9
Figure S6. Cyclic voltammograms of 1b , 2b , 3b with Tetra-n-butyl ammonium chloride	10
CPE leads to the formation of electrochemically active Ru nanoparticles in the bulk solution	11
Figure S7. 1b solution stability test	12
Figure S8. 2b solution stability test	13
Figure S9. 3b solution stability test	14
CPE leads to the formation of electrochemically active Ru nanoparticles on the electrode	15
Figure S10. 1b , 2b , 3b stability at electrode test	16
Figure S11. 1b , 2b , 3b stability tested with HPLC	17
Figure S12. TEM of 2b degradation products	18
Figure S13. Cyclic voltammograms of 0.5mM 3b with different Ar saturation	19
Figure S14. Cyclic voltammograms at differing concentrations 1b	19

Figure S15. Proposed mechanism for 1b and 2b	20
Photochemical formation of Ru nanoparticles	20
Table S2. Turnover numbers for the production of CO, at different times for compounds 1b with and without Hg	21
Table S3. Turnover numbers for the production of H ₂ , CO, and HCCOH at different times for compounds 1b , 2b , and 3b	21
Isotope labeling experiment for clarifying off carbon source of CO production	22
Table S4. Peak area at different times for compound 1b with ¹³ CO ₂	23
Table S5. Normalized absorbance values for compound 1b ¹³ CO ₂	23
Figure S16. ¹ H NMR of <i>fac</i> -[RuCl(dmsO) ₃ (pzH)], 1a , (CD ₃) ₂ CO, r.t.	24
Figure S17. ¹ H NMR of <i>fac</i> -[RuCl(dmsO) ₃ (indzH)], 1b , (CD ₃) ₂ CO, r.t.	24
Figure S18. ¹ H NMR of <i>fac</i> -[RuCl(dmsO) ₃ (NH=C(Me)pz-κ ² N,N)](OTf), 2a , (CD ₃) ₂ CO, r.t.	25
Figure S19. ¹ H NMR of <i>fac</i> -[RuCl(dmsO) ₃ (NH=C(Me)indz-κ ² N,N)](OTf), 2b , (CD ₃) ₂ CO, r.t.	25
Figure S20. ¹ H NMR of <i>fac</i> -[RuCl(dmsO) ₃ (NH=C(Ph)pz-κ ² N,N)](OTf), 3a , (CD ₃) ₂ CO, r.t.	26
Figure S21. ¹ H NMR of <i>fac</i> -[RuCl(dmsO) ₃ (NH=C(Ph)indz-κ ² N,N)](OTf), 3b , (CD ₃) ₂ CO, r.t.	26

Table S1. Electrochemical data obtained by cyclic voltammetry in this study, in DMF and Bu₄PF₆ supporting electrolyte, and referenced to the redox system ferrocenium/ferrocene.^a

Complex	Observed E _{pc} values ^b (Cathodic scan)	i _p (N ₂) ^c (at E _{pc})	i _{cat} (CO ₂) ^c (at E _{pc})	Ratio ^d $\frac{i_{cat}(CO_2)}{i_p(N_2)}$
1a	-2.21,-2.91 ^e	23.0	-43.3	1.88
1b	-2.26,-2.91	20.4	56.5	2.77
2a	-2.10,-2.41, -2.98 ^e	10.7	34.8	3.25
2b	-1.90,-2.53, -2.99 ^e	12.7	36.1	2.84
3a	-2.31,-3.00 ^e	17.8	43.2	2.43
3b	-2.68	23.6	239	10.1

^a The reduction potential mean value observed for Ferrocenium/Ferrocene (Fc⁺/Fc) used as internal calibrant under the employed experimental conditions was E⁰ = 0.443±0.005 V vs. the AgCl/Ag (3M NaCl) electrode.

^b Cathodic scan peaks observed under N₂ unless stated otherwise.

^c Maximum registered cathodic current (μA) under N₂, i_p(N₂), or under CO₂, i_{cat}(CO₂) taken from peak showing greatest enhancement with CO₂ addition.

^d Ratio between the Faradaic currents observed under N₂, i_p(N₂), or under CO₂, i_{cat}(CO₂).

^e Waves where both peaks i_{ox} and i_{red} were observed. Value of E_{1/2} is given in those cases.

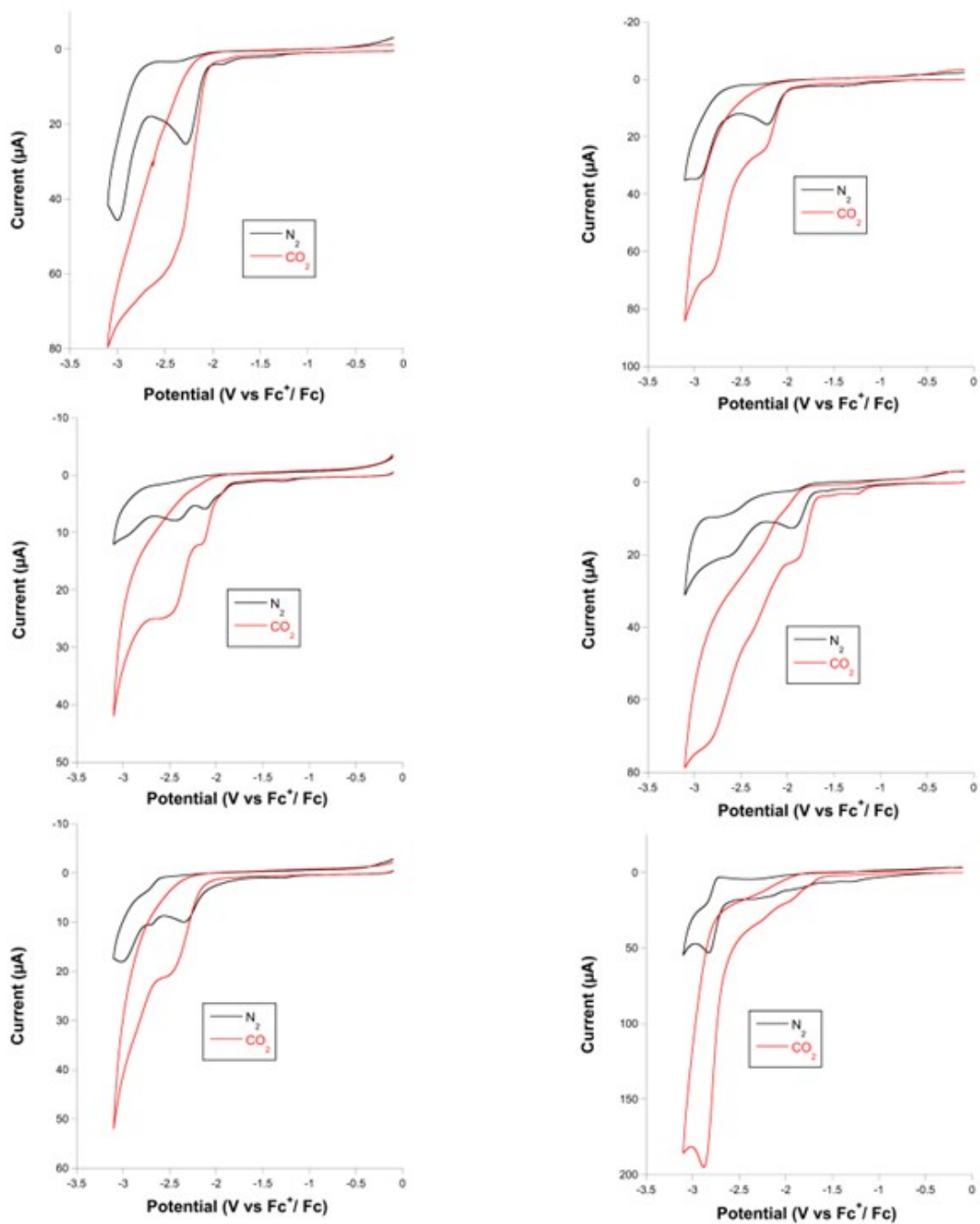


Figure S1. Cyclic voltammograms of all complexes. 1mM complex (glassy carbon working electrode dish 3.0 mm diameter, dry acetonitrile, 0.1 M Bu_4NPF_6) bubbling N_2 (Black) / CO_2 (Red) to the sample, scan rate: 100 mVs^{-1} . Top left **1a**, top right **1b**, middle left **2a**, middle right **2b**, bottom left **3a**, and bottom right **3b**.

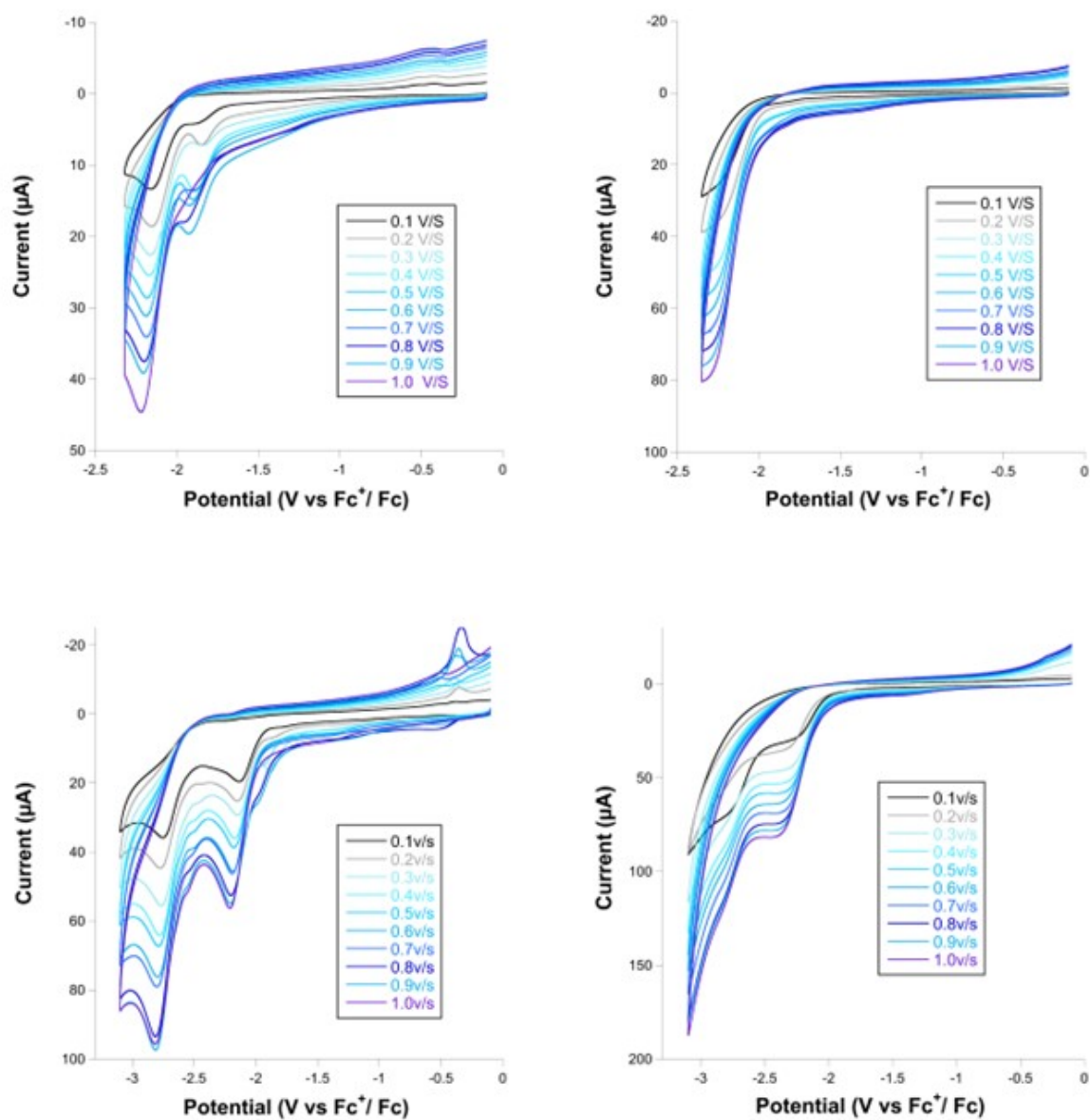


Figure S2. Cyclic voltammograms scan rates complex 1b. 1mM complex (glassy carbon working electrode dish 3.0 mm diameter, dry acetonitrile, 0.1 M Bu₄NPF₆). Top left first electron addition under N₂ atmosphere, top right first electron addition under CO₂ atmosphere, bottom left second electron addition under N₂ atmosphere, and bottom right second electron addition under CO₂ atmosphere.

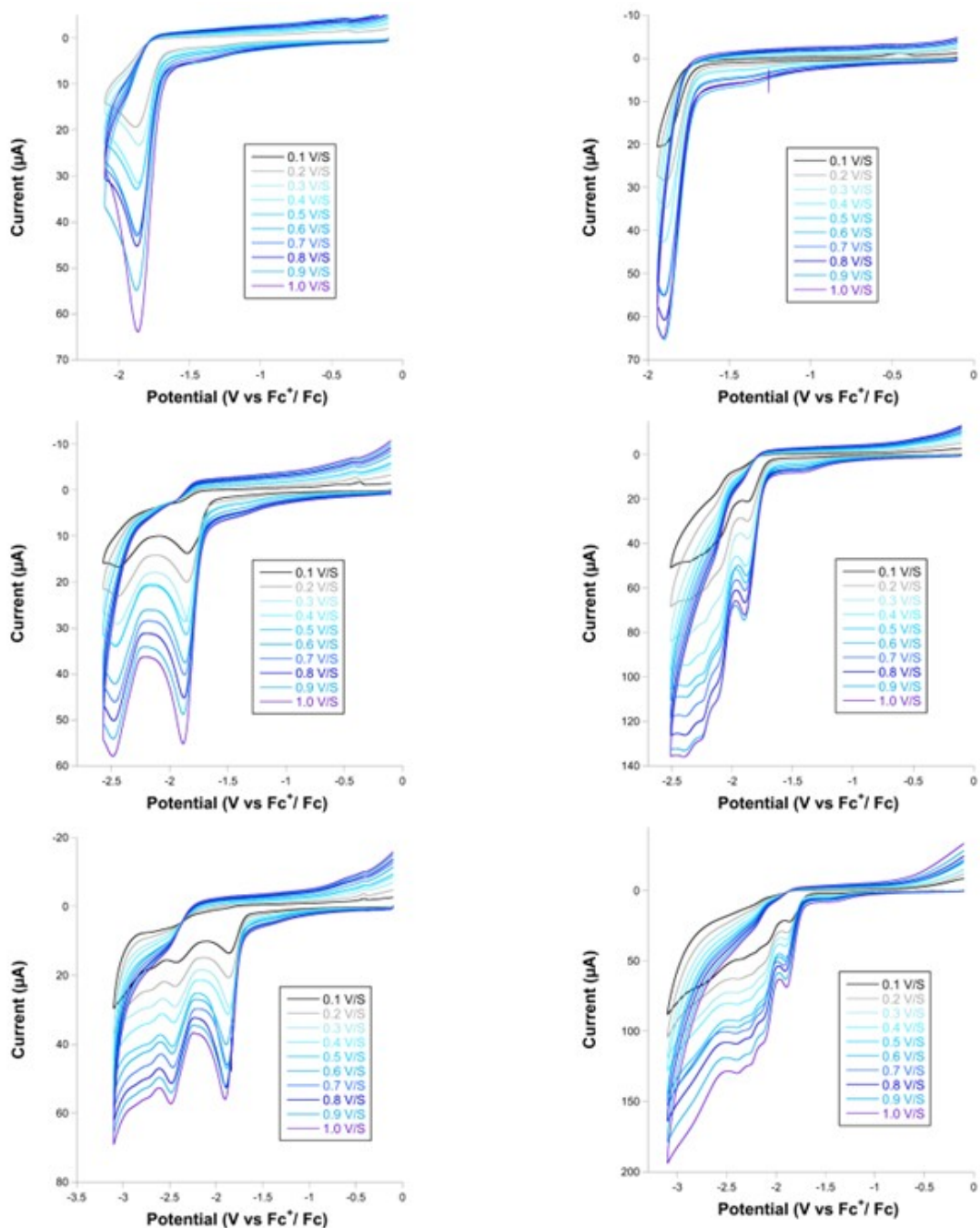


Figure S3. Cyclic voltammograms scan rates complex 2b. 1mM complex (glassy carbon working electrode dish 3.0 mm diameter, dry acetonitrile, 0.1 M Bu₄NPF₆). Top left first electron addition under N₂ atmosphere, top right first electron addition under CO₂ atmosphere, middle left second electron addition under N₂ atmosphere, middle right second electron addition under CO₂ atmosphere, and bottom left third electron addition under N₂ atmosphere, and bottom right third electron addition under CO₂ atmosphere.

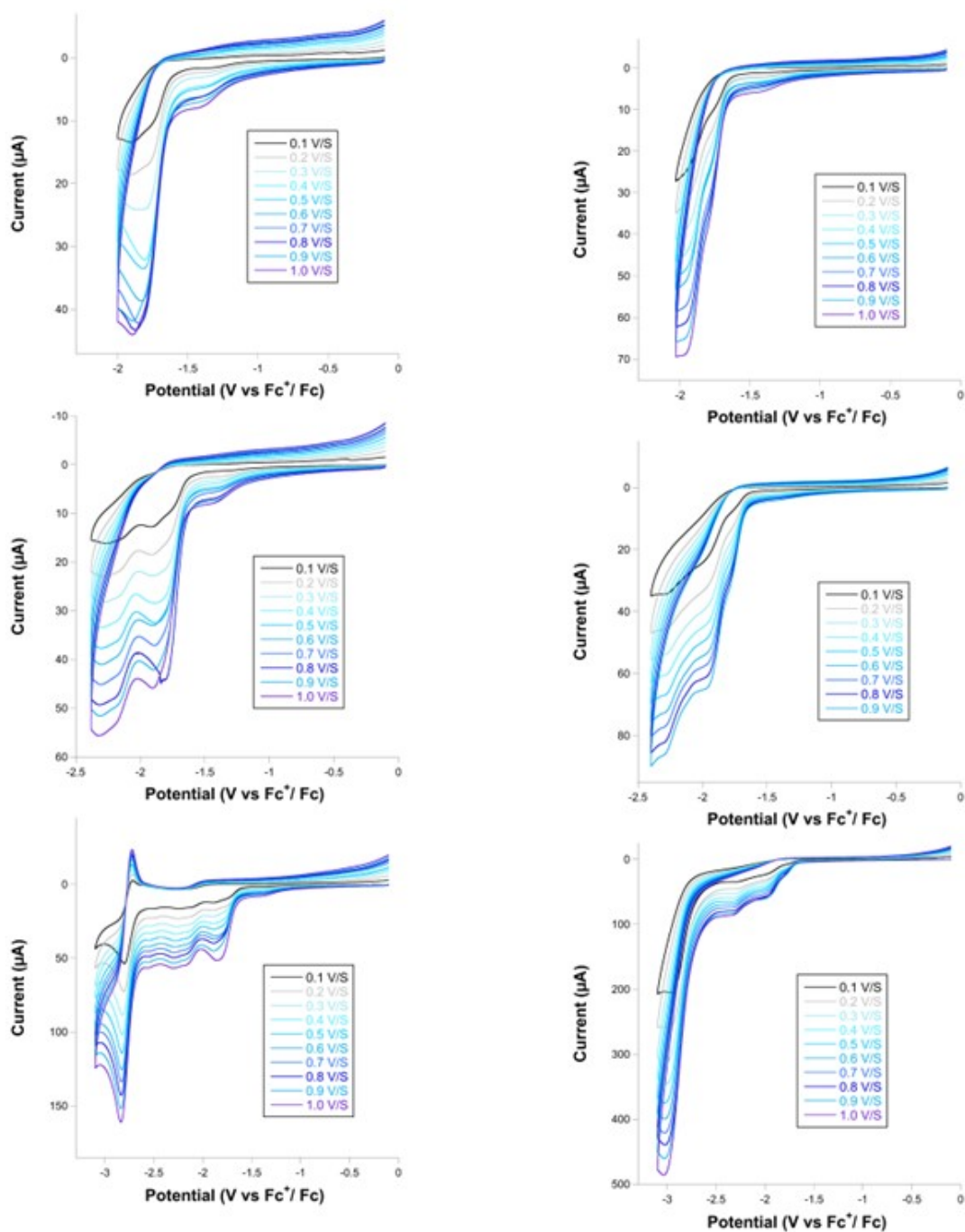


Figure S4. Cyclic voltammograms scan rates complex 3b. 1mM complex (glassy carbon working electrode dish 3.0 mm diameter, dry acetonitrile, 0.1 M Bu₄NPF₆). Top left first electron addition under N₂ atmosphere, top right first electron addition under CO₂ atmosphere, middle left second electron addition under N₂ atmosphere, middle right second electron addition under CO₂ atmosphere, and bottom left third electron addition under N₂ atmosphere, and bottom right third electron addition under CO₂ atmosphere.

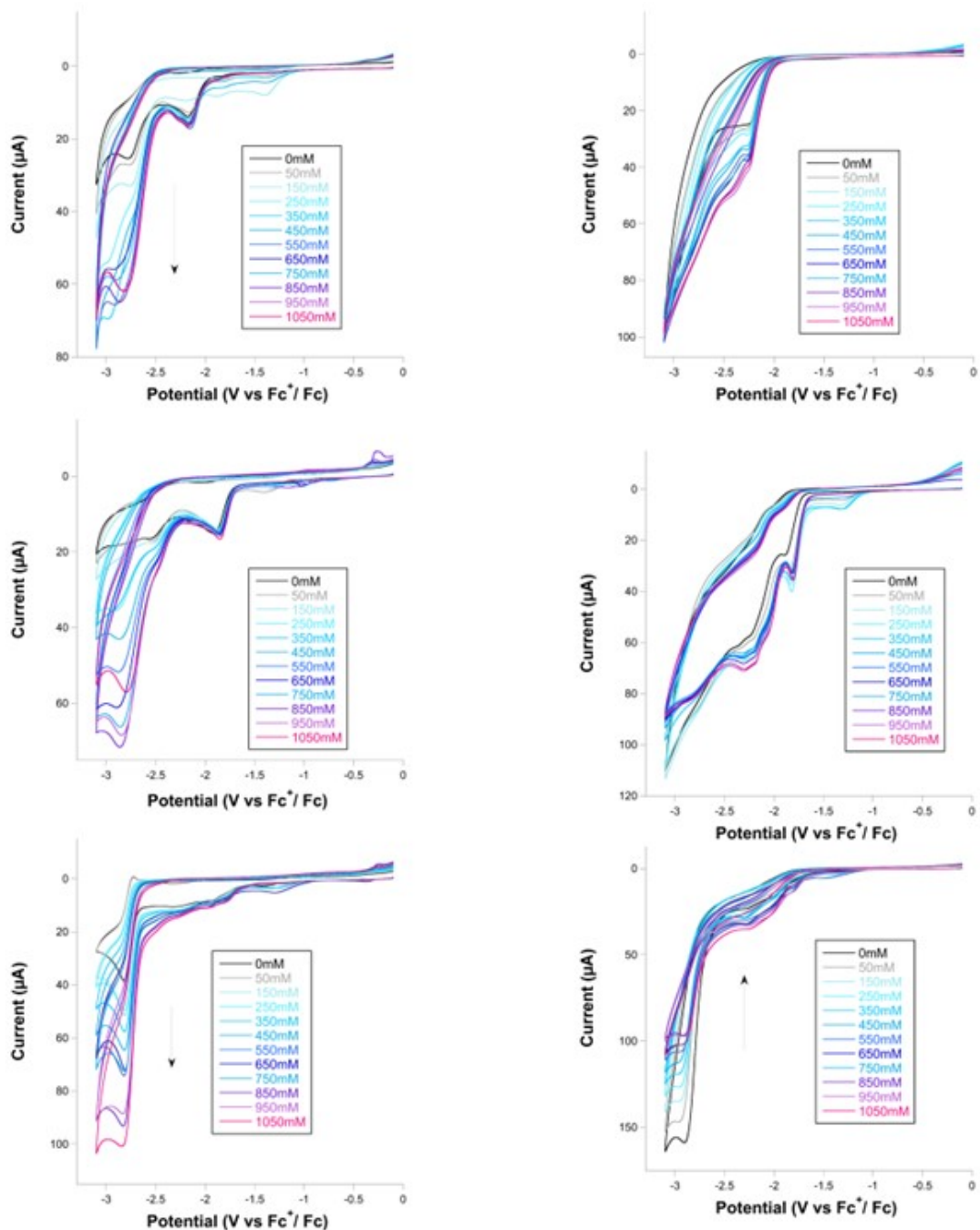


Figure S5. Cyclic voltammograms of **1b**, **2b**, **3b** with proton source. 1mM complex (glassy carbon working electrode dish 3.0 mm diameter, dry acetonitrile, 0.1 M Bu_4NPF_6), scan rate: 100 mVs^{-1} with varying H_2O concentrations from 0mM to 1050mM. Top left **1b** under N_2 atmosphere, top right **1b** under CO_2 atmosphere, middle left **2b** under N_2 atmosphere, middle right **2b** under CO_2 atmosphere, and bottom left **3b** under N_2 atmosphere, and bottom right **3b** under CO_2 atmosphere.

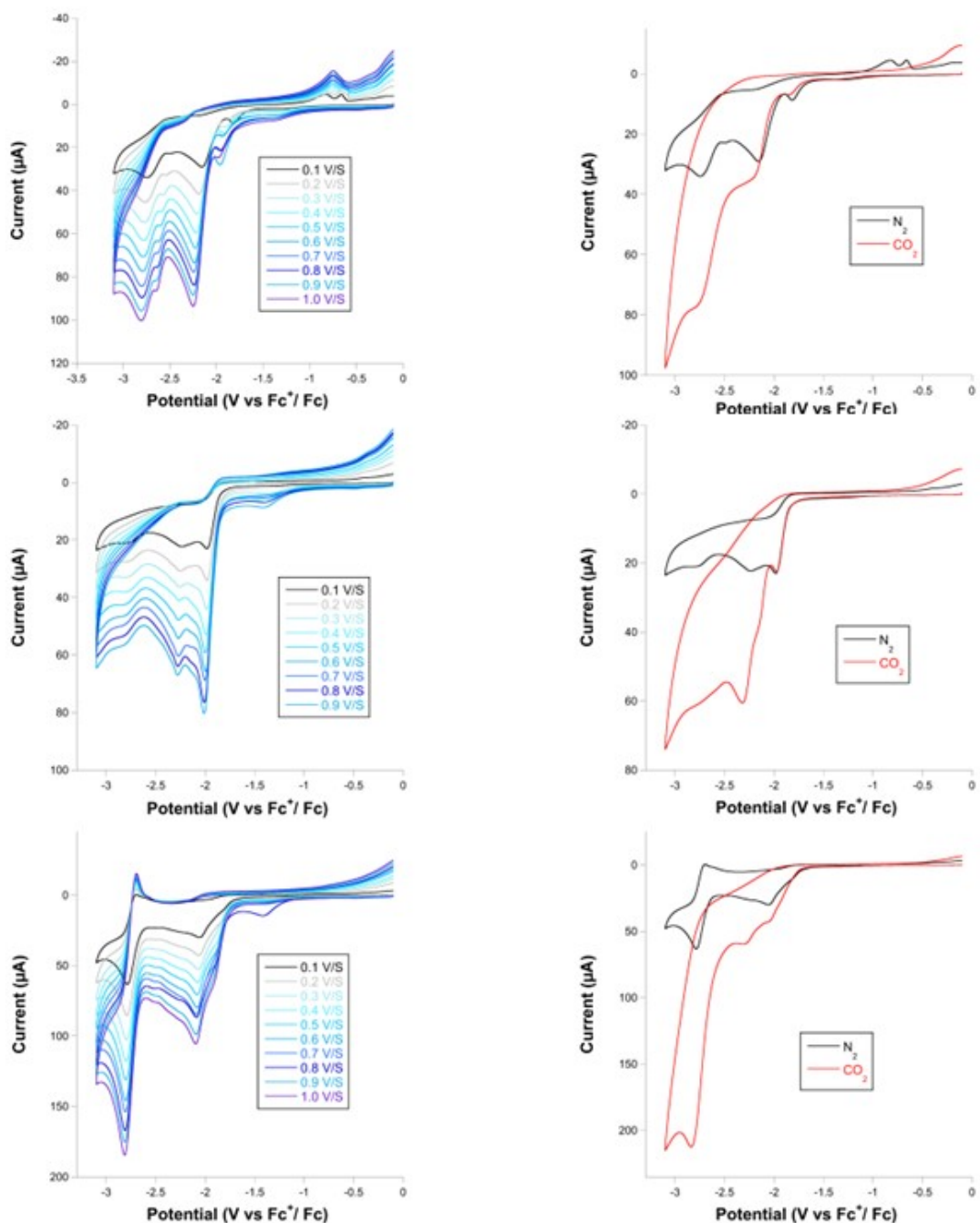


Figure S6. Cyclic voltammograms of **1b**, **2b**, **3b** with TBACl. 1mM complex (glassy carbon working electrode dish 3.0 mm diameter, dry acetonitrile, 0.1 M Bu₄NCl). Top left **1b** under N₂ atmosphere varying scan rate, top right **1b** under CO₂/ N₂ atmosphere, middle left **2b** under N₂ atmosphere varying scan rate, middle **2b** under CO₂/ N₂ atmosphere, and bottom left **3b** under N₂ atmosphere varying scan rate, **3b** under CO₂/ N₂ atmosphere.

Controlled potential electrolysis (CPE) leads to the formation of electrochemically-active Ruthenium nanoparticles in the bulk solution.

We tested the hypothesis that Ru(0) nanoparticle could form under electrochemical conditions. Their role in the catalytic system was tested by running CPE for four hours, and then performing cyclic voltammetric experiments on samples pulled from the CPE.

A 25 mL solution of dry acetonitrile with 1.0 mM **1b,2b**, or **3b**, 0.1 M Bu₄NPF₆, was prepared in a cell with a glassy carbon rod working electrode, Pt counter electrode and Ag/AgCl reference electrode. A controlled potential electrolysis experiment was run at run at -2.4 V to -2.7 (vs Fc⁺/Fc) depending on whichever electron addition showing the greatest enhancement with the addition of CO₂ as previously determined by CV for 4 hours while the solution was under CO₂ atmosphere and stirring. Samples of the 25 mL solution were pulled and tested with cyclic voltammetry at 0 h, 2 h, and 4 hours (Figure S7-9) under CO₂ atmosphere, using a glassy carbon working electrode dish 3.0 mm diameter, and a scan rate of 100 mVs⁻¹, then bubbled N₂ for 15 minutes and the scan was repeated. After the 4 h scans were completed, 10 equivalents of Hg(I) was added and allowed to stir for 8h under N₂ atmosphere, after which time cyclic voltammetry CO₂ and N₂ were preformed using the previously stated conditions. Over time a large increase in activity can be seen both under N₂, along with a smaller increase to CO₂, this is due to the degradation of the 2b molecular catalysis in solution. Two degradation products are being formed one the active molecular catalyst which has yet to be characterized and the other a further degradation to a Ruthenium nanoparticle. At the four hour time point the CO₂ and N₂ voltammograms homogenize showing that the predominant species in the solution is able to accept electrons however not catalytically reduce CO₂. At this point the Hg was added to the solution to test if the species that was responsible for this activity was a Ruthenium nanoparticles, due to the ability of Hg to bond neutral Ruthenium species. After allowing the Hg to stir with the post BE solution for four hours cyclic voltammetry was preformed once more, with the same conditions as previously stated. The cyclic voltammetry under N₂ starts to return to that of the inithial **1b,2b**, and **3b** solution showing that some of this activity comes from the presence of Ruthenium nanoparticles. Under catalytic conditions it can be seen that there is little change to the activity however the cathodic wave seen around -2.5 V (vs Fc⁺/Fc) returns, due to the molecular a molecular form of **1b,2b**, and **3b** being the predominant searches once more.

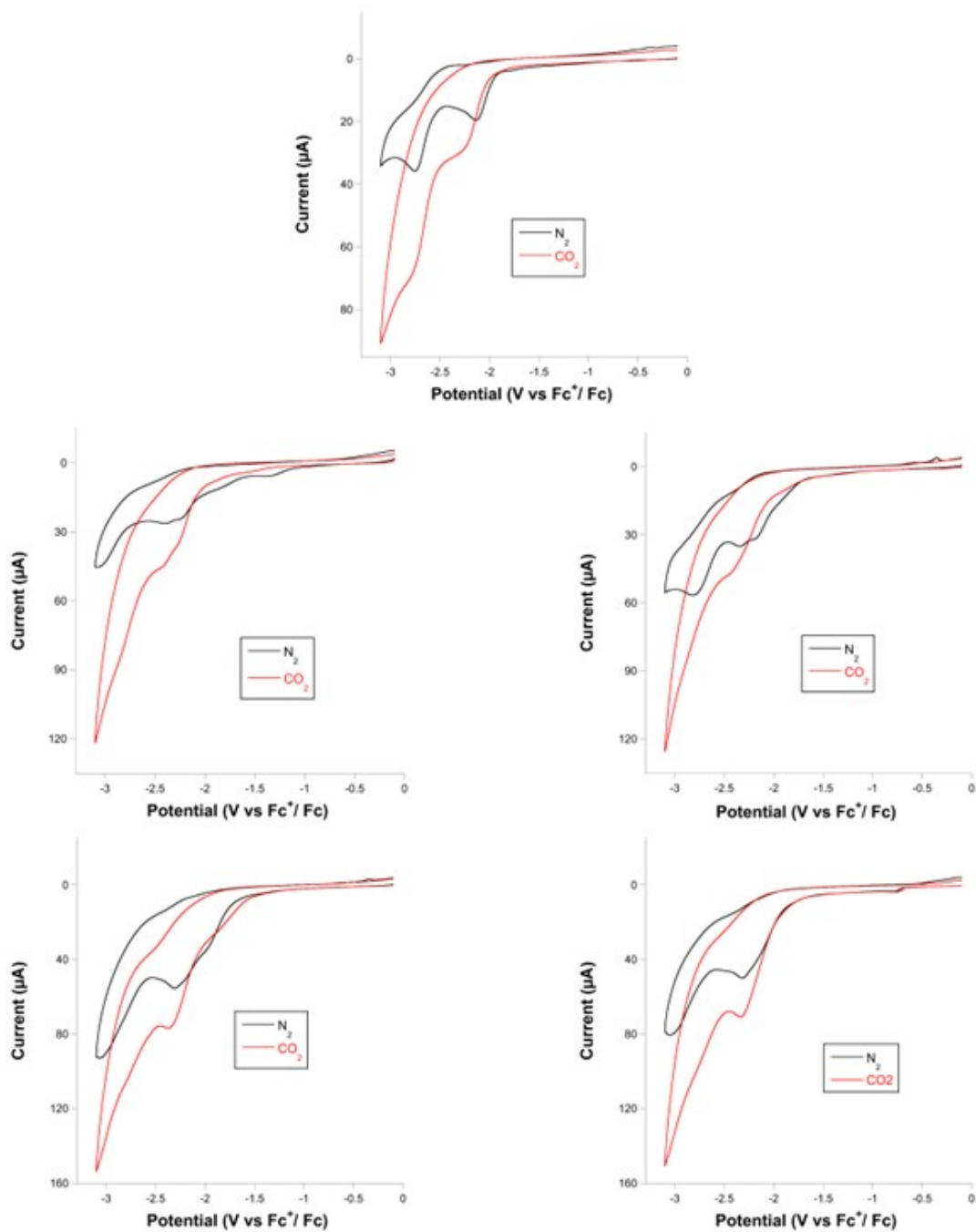


Figure S7. 1b solution stability test. 1mM **1b** (glassy carbon working electrode dish 3.0 mm diameter, dry acetonitrile, 0.1 M Bu₄NPF₆) bubbling N₂(Black) /CO₂(Red) to the sample, scan rate: 100 mVs⁻¹. Top **1b** 0h, middle left **1b** 2h, middle right **1b** 4h, and bottom left **1b** 6h, bottom right **1b** after the addition of Hg.

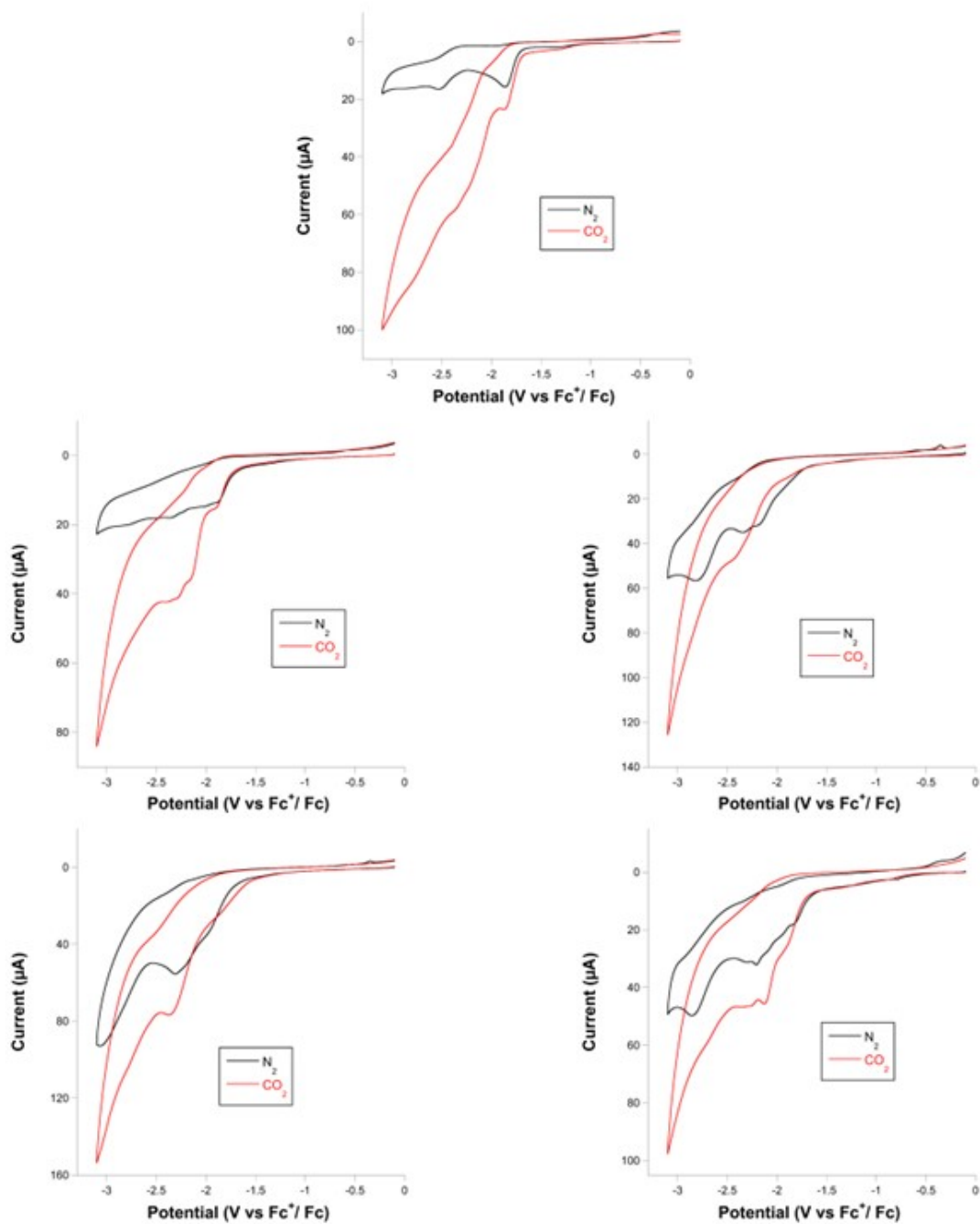


Figure S8. 2b solution stability test. 1mM **2b** (glassy carbon working electrode dish 3.0 mm diameter, dry acetonitrile, 0.1 M Bu₄NPF₆) bubbling N₂(Black) /CO₂(Red) to the sample, scan rate: 100 mVs⁻¹. Top **2b** 0h, middle left **2b** 2h, middle right **2b** 4h, and bottom left **2b** 6h, bottom right **2b** after the addition of Hg.

q

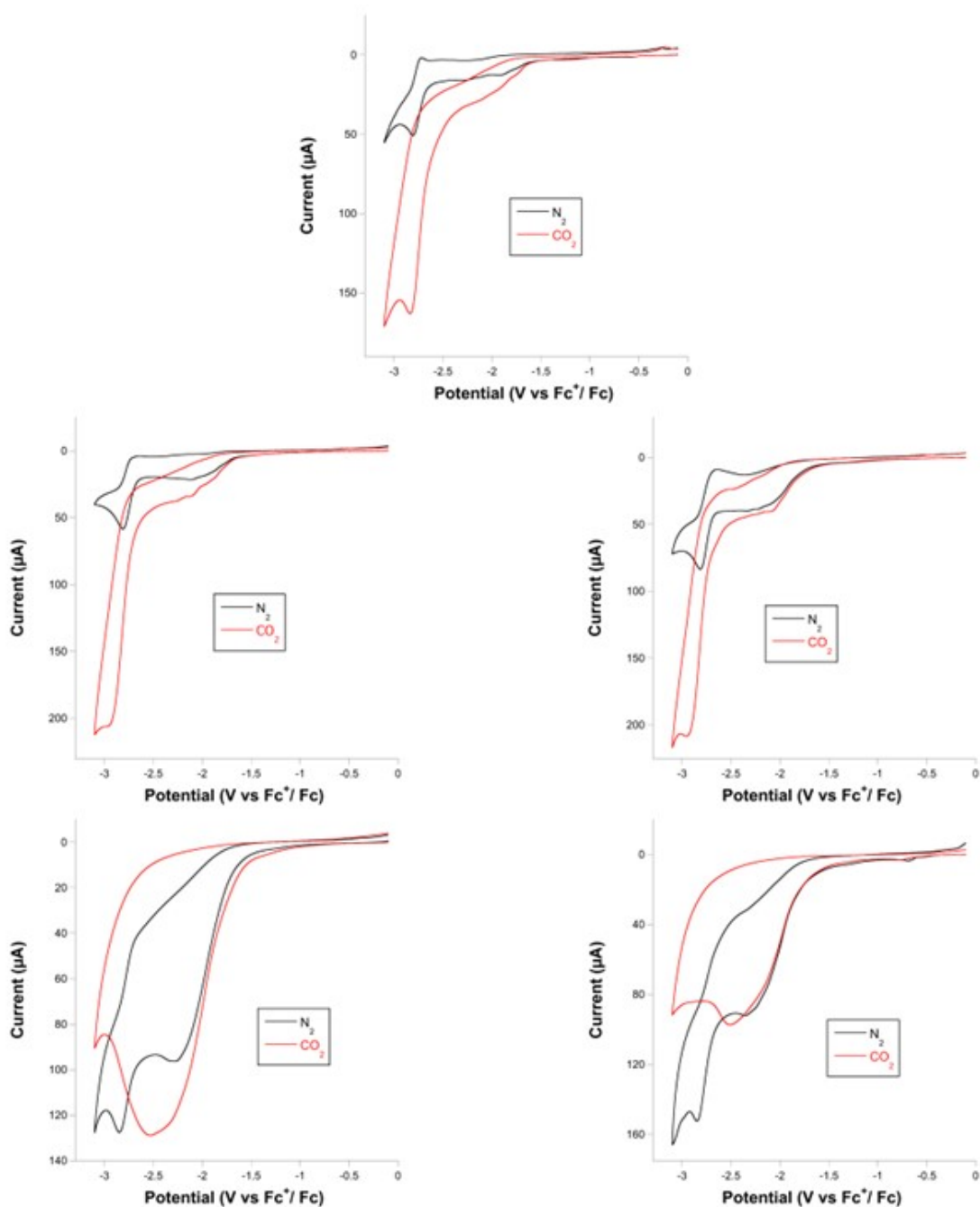


Figure S9. 3b solution stability test. 1mM **3b** (glassy carbon working electrode dish 3.0 mm diameter, dry acetonitrile, 0.1 M Bu₄NPF₆) bubbling N₂(Black) /CO₂(Red) to the sample, scan rate: 100 mVs⁻¹. Top **3b** 0h, middle left **3b** 2h, middle right **3b** 4h, and bottom left **3b** 6h, bottom right **3b** after the addition of Hg.

Controlled potential electrolysis (CPE) leads to the formation of electrochemically -active Ruthenium nanoparticles on the electrode.

We tested the hypothesis that Ru(0) nanoparticle catalysts could form on the electrodes by running CPE for two hours, and then performing cyclic voltametric experiments, first with the electrode “as is”, and then after cleaning the electrode. The results are shown below (Figure S10) and show that a catalytically-active film, probably containing Ru nanoparticles, forms on the electrode. Details of the experiments are also shown below.

A 10 mL solution of dry acetonitrile with 1.0 mM **1b,2b**, or **3b**, 0.1 M Bu₄NPF₆, was prepared in a cell with a glassy carbon working electrode dish 3.0 mm, Pt counter electrode and Ag/AgCl reference electrode. The electrochemical behavior was measured using cyclic voltammetry at a scan rate of 100 mVs⁻¹ under N₂ and CO₂ (T = 0 h, Figure S34). Next, a controlled potential electrolysis was run at -2.4 V to -2.7 (vs Fc⁺/Fc) depending on whichever electron addition showing the greatest enhancement with the addition of CO₂ as previously determined by CV for 2 hours while the solution was under CO₂ atmosphere and stirring. A cyclic voltammetry experiment was performed using the CPE working electrode “as is” with the same conditions as in Figure S10. Clear differences are observed under N₂ and CO₂. Upon observation of the electrode surface, one could see a black particulate on top of the electrode. Further characterization of the black powder was not performed. Finally, the glassy carbon working electrode was cleaned with a small amount of acetonitrile on a wipe, so as to remove any formation on the surface without making any modification to the electrode surface, at which point a cyclic voltammetry was run as before using the solution from the bulk electrolysis. The similarities between the “as is” and “clean” show that most of the compound remains intact in solution, but changes happened on the electrode. The new material builds up on it, leading to a larger electrochemical activity under these conditions. This behavior can be contributed to a buildup of nanoparticle that have the ability to accept electrons at a simpler over potential to the active molecular Ru catalyst. As can be seen from the Hg test run when testing the rruthenium nanoparticles in the bulk solution (Figure S7- Figure S9). It is seen in both the bulk solution test, and now with the electrode surface test with **1b,2b**, and **3b** there is an increased activity under N₂ and CO₂ with the post CPE solution. This shows the formation of nanoparticles that accepting electrodes, however there is likely not full coverage of the electrode surface. This leads to the increase in cathodic current under N₂ and CO₂, which is adding to the cathodic wave seen, blending with the activity of CO₂ reduction that is normally observed for 2b, due to the partial coverage of the electrode surface, allowing for both processes to be observed at once.

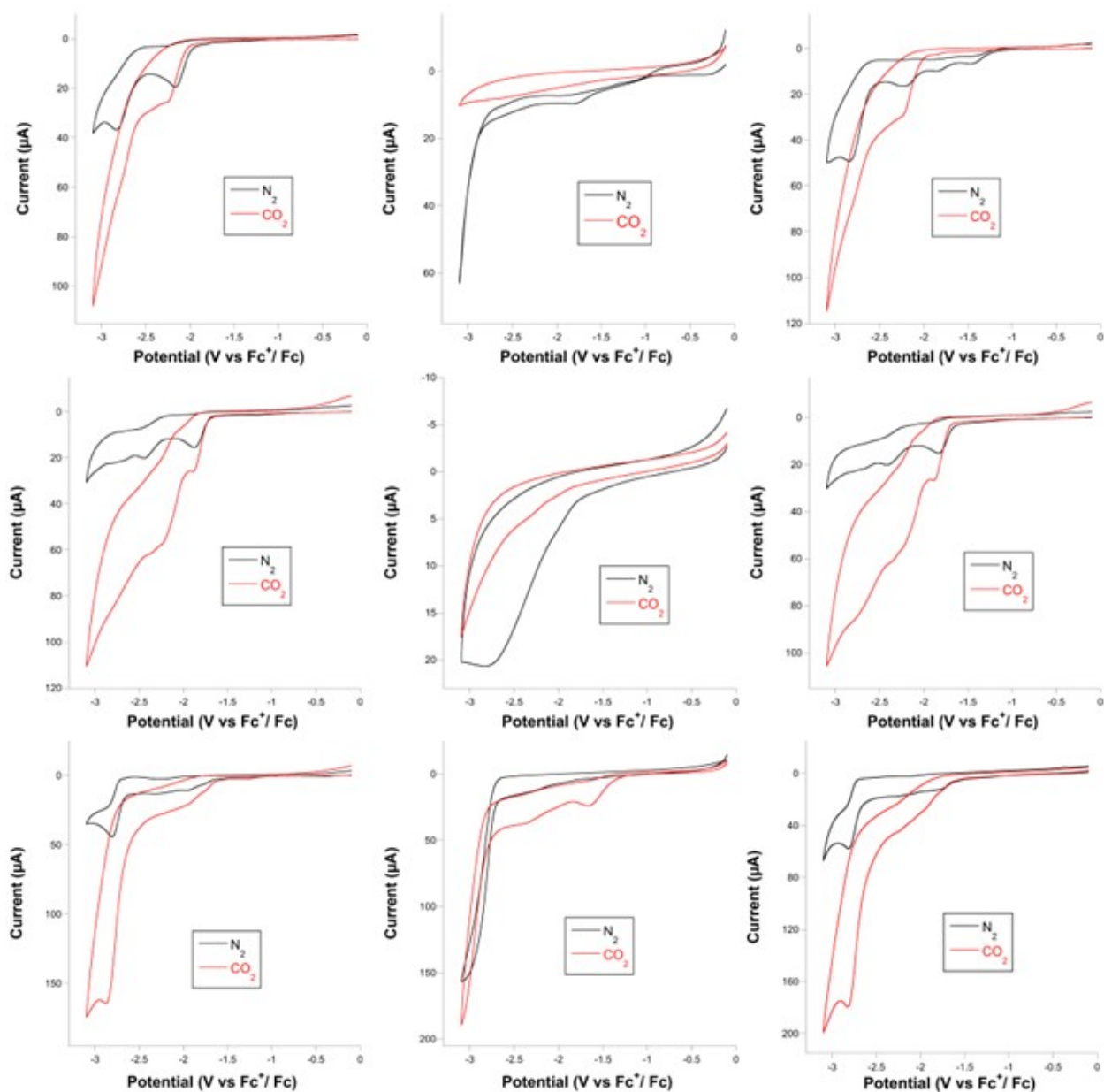


Figure S10. **1b**, **2b**, **3b** stability at electrode test. 1mM catalyst (glassy carbon working electrode dish 3.0 mm diameter, dry acetonitrile, 0.1 M Bu_4NPF_6) bubbling N_2 (Black) / CO_2 (Red) to the sample, scan rate: 100 mVs^{-1} . Top left **1b** 0h, top middle **1b** "as is", top right **1b** "cleaned", middle left **2b** 0h, middle middle **2b** "as is", middle right **2b** "cleaned", bottom left **3b** 0h, bottom middle **3b** "as is", bottom right **3b** "cleaned".

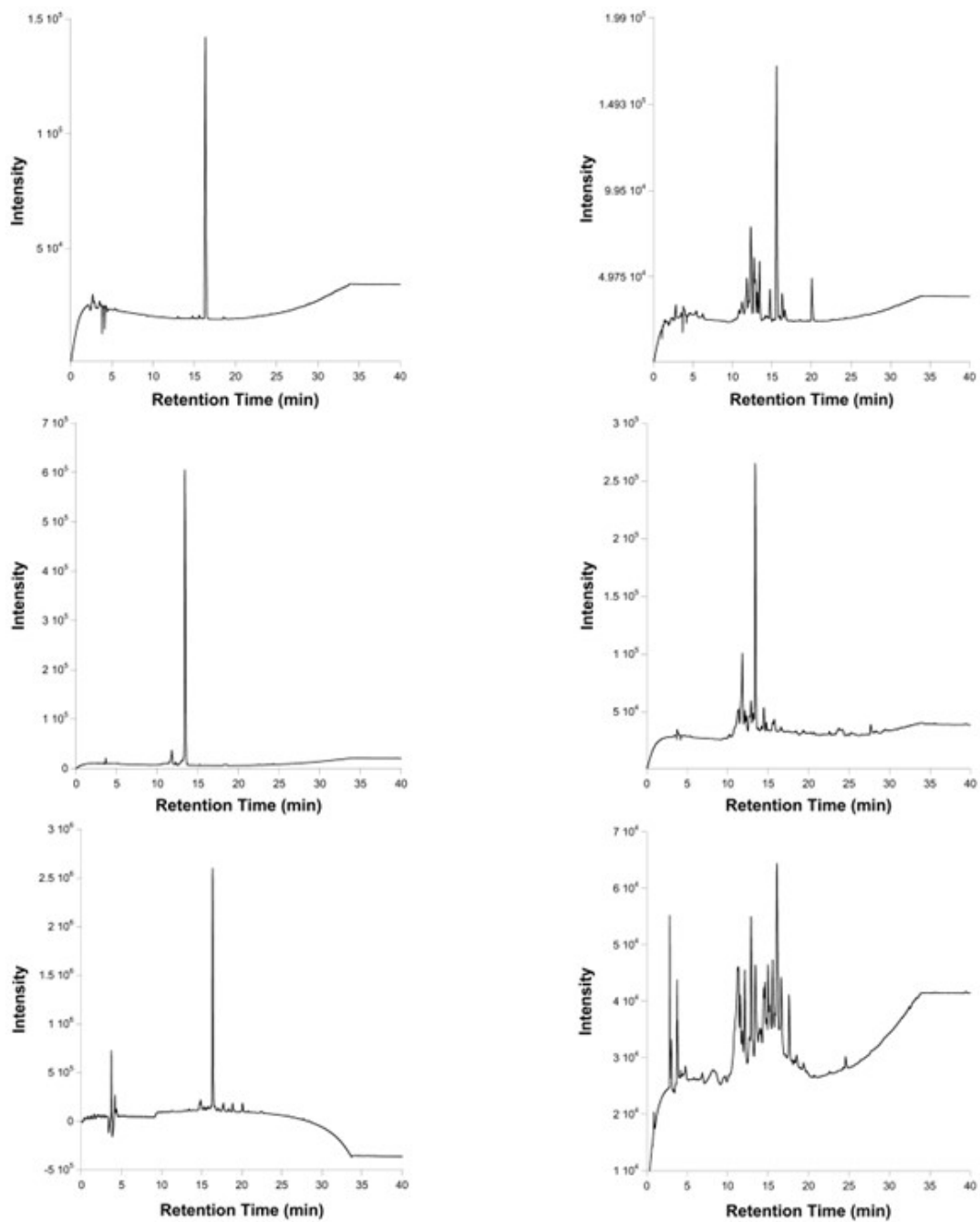
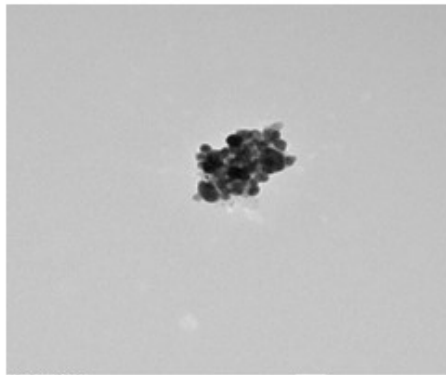
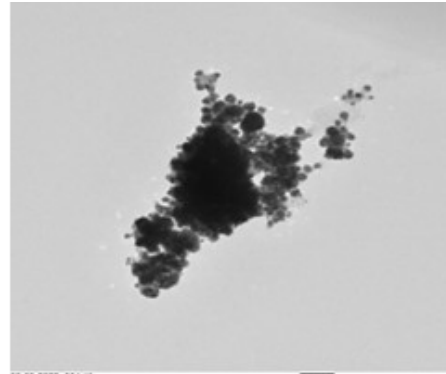


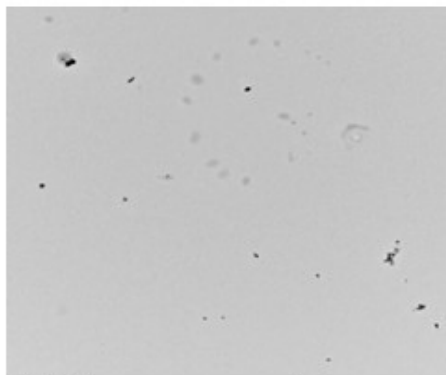
Figure S11. **1b, 2b, 3b** stability tested with HPLC. Aliquots taken from solutions of 1mM catalyst, dry acetonitrile, 0.1 M Bu_4NPF_6 . Top left **1b** pre BE, top right **1b** post BE, middle left **2b** pre BE, middle right **2b** post BE, bottom left **3b** pre BE, bottom right **3b** post BE.



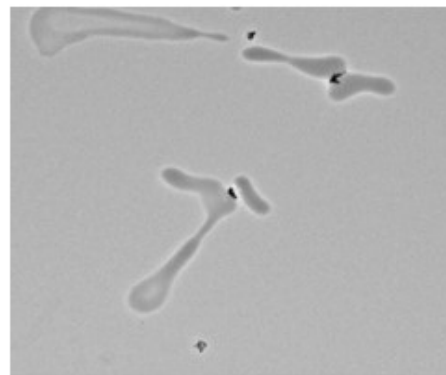
09-09-2023_261.tif
Murphy's sample
50 nm
HV=120kV
Direct Mag: 120000 x
AMT Camera System
Camera: NANOSPR12, Exposure: 400 (ms) x 4 000 frames, Gain: 3, Bin: 1
Gain: 1.00, No Sharpening, Normal Contrast



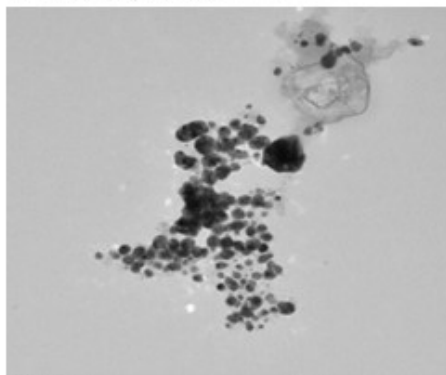
09-09-2023_264.tif
Murphy's sample
100 nm
HV=120kV
Direct Mag: 60000 x
AMT Camera System
Camera: NANOSPR12, Exposure: 400 (ms) x 4 000 frames, Gain: 3, Bin: 1
Gain: 1.00, No Sharpening, Normal Contrast



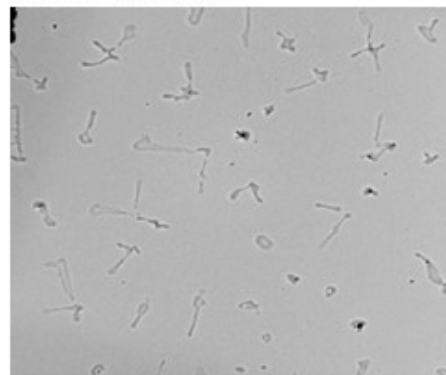
09-09-2023_262.tif
Murphy's sample
1 µm
HV=120kV
Direct Mag: 6000 x
AMT Camera System
Camera: NANOSPR12, Exposure: 400 (ms) x 4 000 frames, Gain: 3, Bin: 1
Gain: 1.00, No Sharpening, Normal Contrast



09-09-2023_265.tif
Murphy's sample
500 nm
HV=120kV
Direct Mag: 12000 x
AMT Camera System
Camera: NANOSPR12, Exposure: 400 (ms) x 4 000 frames, Gain: 3, Bin: 1
Gain: 1.00, No Sharpening, Normal Contrast



09-09-2023_263.tif
Murphy's sample
50 nm
HV=120kV
Direct Mag: 120000 x
AMT Camera System
Camera: NANOSPR12, Exposure: 400 (ms) x 4 000 frames, Gain: 3, Bin: 1
Gain: 1.00, No Sharpening, Normal Contrast



09-09-2023_266.tif
Murphy's sample
2 µm
HV=120kV
Direct Mag: 2900 x
AMT Camera System
Camera: NANOSPR12, Exposure: 400 (ms) x 4 000 frames, Gain: 3, Bin: 1
Gain: 1.00, No Sharpening, Normal Contrast

Figure S12 TEM of 2b degradation products.

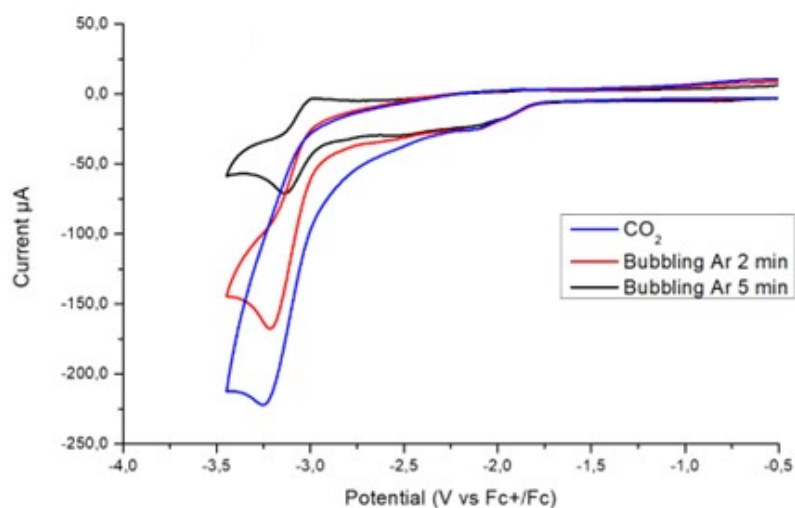


Figure S13. Cyclic voltammograms of 0.5mM 3b with different Ar saturation. (glassy carbon working electrode dish 3.0 mm diameter, dry acetonitrile, 0.1 M Bu_4NPF_6) bubbling Ar to the sample in CO_2 atmosphere, scan rate: 100 mVs^{-1} .

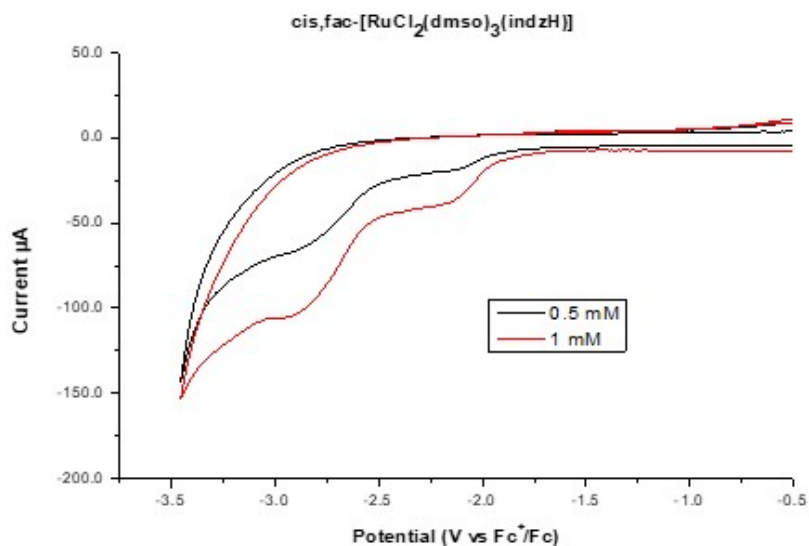


Figure S14. Cyclic voltammograms of 0.5mM 1b. (glassy carbon working electrode dish 3.0 mm diameter, dry acetonitrile, 0.1 M Bu_4NPF_6) under CO_2 at different concentrations of 1b.

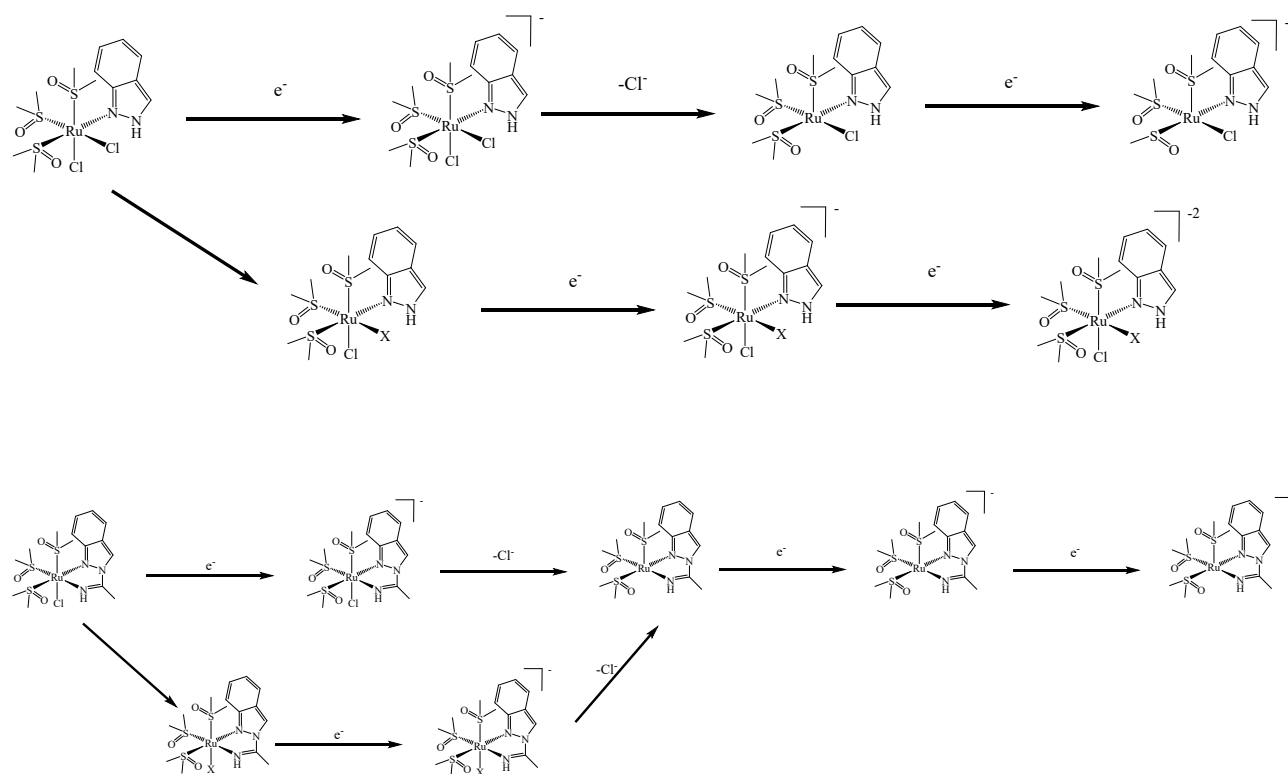


Figure S15. Proposed mechanisms for **1b** (above) and **2b** (below)

Photochemical formation of Ruthenium nanoparticles

We tested the hypothesis that Ru(0) nanoparticle could form under photochemical conditions. First a pair of controls were run both containing; 1.6 mM [Ru(3-isoquinoline)(bipy)₂] (isopic), and 100 mM 1,3-dimethyl-2-phenyl-2,3-dihydro-1H-benzo[d]imidazole (BIH), along with one containing 10mM Hg. They were all irradiated with white light greater than 300nm, for times 2,6, and 24 hours. At each time point a 500ml sample was injected into a gas chromatographer and quantified, as described in the experimental segment of the paper. In the table turnover numbers (TON) for the production of CO are given as a measure of activity of the samples. For the first two TON is calculated in comparison to isopic due to it being the only likely source of CO₂ reduction. Next two samples are run using the same conditions as the controls except now one of the “b” compound was added, The sample with the Hg present show little to no effect on the TON compared to the sample without. This is evidence to support that Ruthenium nanoparticles maybe present in the solution however are not the active catalyst.

Table S2. Turnover numbers for the production of CO, at different times for compounds 1b with and without Hg.

Time (h)	Control	Control + Hg	1b	1b + H ₂ O	1b + Hg	2b	2b + H ₂ O	2b Hg	3b	3b + H ₂ O	3b + Hg
2	0.2	0.3	61.8	63.1	8.0	37.6	30.8	13.0	16.3	14.2	20.1
6	0.2	0.3	87.3	87.1	18.9	53.1	36.5	11.7	32.1	27.2	33.3
24	0.2	0.3	141.5	145.1	39.7	104.9	51.4	23.4	64.7	55.0	73.7

Turnover number CO evolved from CO₂-saturated solutions irradiated by >300 nm visible light with 10mM Hg when specified. "control" contains 1.6 mM [Ru(3-isoquinoline)(bipy)₂] (isopic), 100 mM 1,3-dimethyl-2-phenyl-2,3-dihydro-1H-benzo[d]imidazole (BIH). All samples contain the "control" solution with the addition of one of the complexes as well as H₂O or Hg.

Table S3. Turnover numbers for the production of H₂, CO, and HCCOH at different times for compounds 1b, 2b, and 3b.

Time (h)	1b TON H ₂	1b TON CO	1b TON HCOOH	2b TON H ₂	2b TON CO	2b TON HCOOH	3b TON H ₂	3b TON CO	3b TON HCOOH
2	467	116	0.370	312	60.2	0.551	186	52.9	0.318
4	593	144	-	371	77.3	-	418	96.8	-
6	616	138	-	330	59.5	-	403	85.6	-
8	713	169	-	585	135	-	402	92.9	-
12	590	113	0.717	626	114	0.664	425	100	0.732

Turnover number CO and H₂ evolved from 0.1 mM Ru complexes, 1.6 mM [Ru(bipy)₃]²⁺ in a CO₂-saturated MeCN-TEOA solution (4:1 v/v) irradiated by >300 nm visible light.

Isotope labeling experiment for clarifying off carbon source of CO production.

We tested the hypothesis that the CO produced from the Ru catalysts **1b**, **2b**, **3b**, was due to their consumption of available CO₂ which is saturated into the solution and not due to the degradation of other species. In order to do this a photochemical experiment was carried out where a control solution of 1.6 mM [Ru(3-isoquinoline)(bipy)₂] (isopic), 100 mM 1,3-dimethyl-2-phenyl-2,3-dihydro-1H-benzo[d]imidazole (BIH) in dry MeCN, and then a solution of isopic and BIH with **1b** in dry MeCN were prepared in sealed glass tubes and tested with GC as well as GC coupled MS. Both solutions were purged with N₂ for 10 min, then degassed with freeze thaw cycles three times, before being saturated with ¹³CO₂. At which time solutions, were irradiated by >300 nm visible light. A 500 μl injection from the headspace of the reaction vessel was injected into the GC to acquire the peak areas for N₂, CO, and CO₂ at both times 0h and 24h, the same was done for the GC MS. The GC data to understand the amount of each gas present. Were as the GC MS to understand the isotopes of the gases. For the control it can be seen that the amount of N₂, CO, and CO₂ are consistent throughout the experiment showing no CO₂ catalysis is taking place or degradation of the solution into CO. When the control is run in the GC MS it is seen that the peak at 24 m/z which contains N₂ as well as ¹²CO is consistent along with the peak at 45 m/z for ¹³CO₂. For the sample solution it can be seen that the amount of N₂ is consistent throughout the experiment, whereas the amount of CO₂ is decreased proportionally to the increase of CO. When the sample is run in the GC MS it is seen that the peak at 24 m/z which contains N₂ as well as ¹²CO is consistent whereas there is now a peak at 25 m/z for ¹³CO along with the peak at 45 m/z for ¹³CO₂ now decreasing. Showing that the CO that is being produced in this experiment is primarily if not interlay sourced from the CO₂.

Table S4. Peak area at different times for compound **1b** with $^{13}\text{CO}_2$.

Time (h)	N ₂ Control	CO Control	CO ₂ Control	N ₂ Sample	CO Sample	CO ₂ Sample
0	494557	0	713591	88164	0	1700876
24	518868	0	732270	88164	256471	1309153

Peak area of CO evolved from $^{13}\text{CO}_2$ -saturated solutions irradiated by >300 nm visible light with 1.6 mM [Ru(3-isoquinoline)(bipy)₂] (isopic), 100 mM 1,3-dimethyl-2-phenyl-2,3-dihydro-1H-benzo[d]imidazole (BIH), for "control". "Sample" also irradiated by >300 nm visible light with 1.6 mM [Ru(3-isoquinoline)(bipy)₂] (isopic), 100 mM 1,3-dimethyl-2-phenyl-2,3-dihydro-1H-benzo[d]imidazole (BIH), and **1b**.

Table S5. Normalized absorbance values for compound **1b** $^{13}\text{CO}_2$

	28 m/z	29 m/z	44 m/z	45 m/z
Control (0h)	3.1	1.0	0	2.3
Control (24h)	2.9	1.0	0	2.6
Sample (0h)	0.8	1.0	0	2.3
Sample (24h)	1.0	2.1	0	2.4

Absorbance values from 500 μl injection to GC-MS of a $^{13}\text{CO}_2$ -saturated solutions irradiated by >300 nm visible light with 1.6 mM [Ru(3-isoquinoline)(bipy)₂] (isopic), 100 mM 1,3-dimethyl-2-phenyl-2,3-dihydro-1H-benzo[d]imidazole (BIH), for "control". "Sample" also irradiated by >300 nm visible light with 1.6 mM [Ru(3-isoquinoline)(bipy)₂] (isopic), 100 mM 1,3-dimethyl-2-phenyl-2,3-dihydro-1H-benzo[d]imidazole (BIH), and **1b**. All absorbance values normalized to the value of the 29 m/z for control (0h) (1400,000).

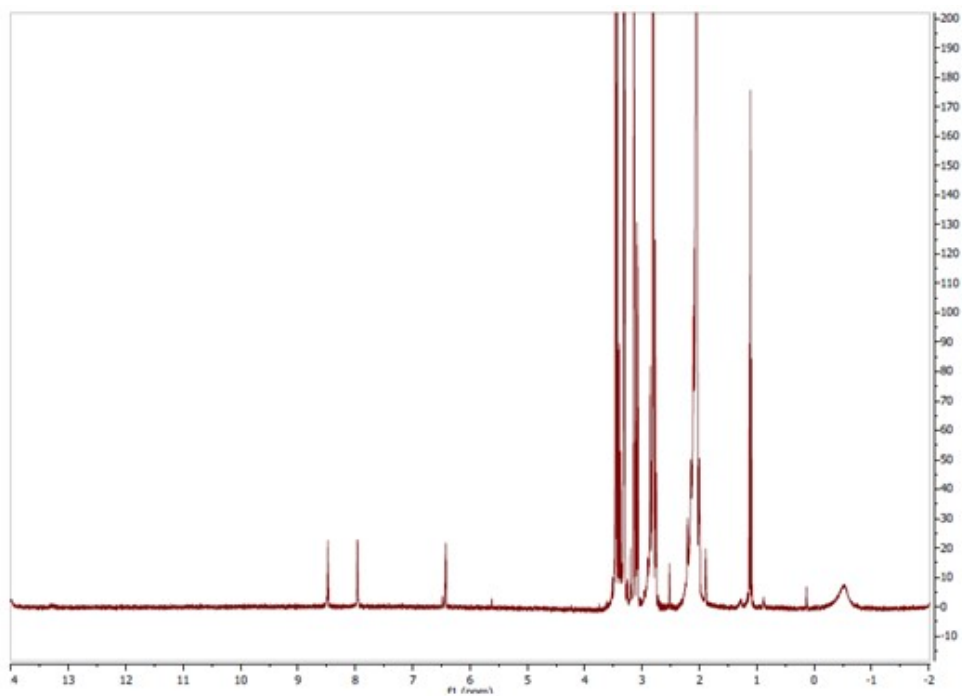


Figure S16. ^1H NMR of $\text{fac-}[\text{RuCl}(\text{dmsO})_3(\text{pzH})]$, **1a**, $(\text{CD}_3)_2\text{CO}$, r.t.

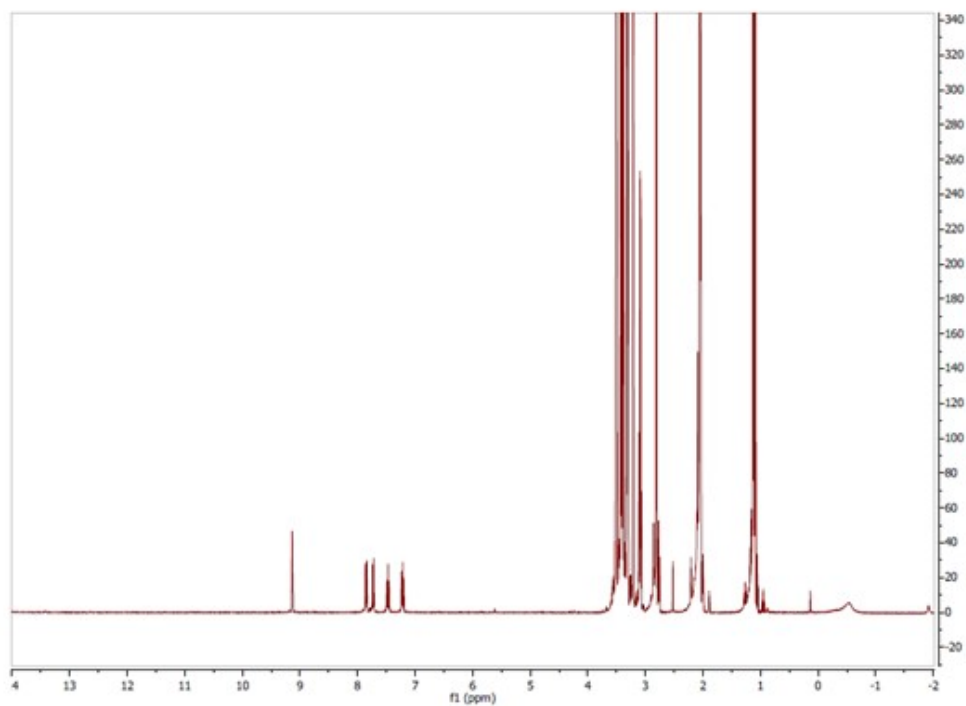


Figure S17. ^1H NMR of $\text{fac-}[\text{RuCl}(\text{dmsO})_3(\text{indzH})]$, **1b**, $(\text{CD}_3)_2\text{CO}$, r.t.

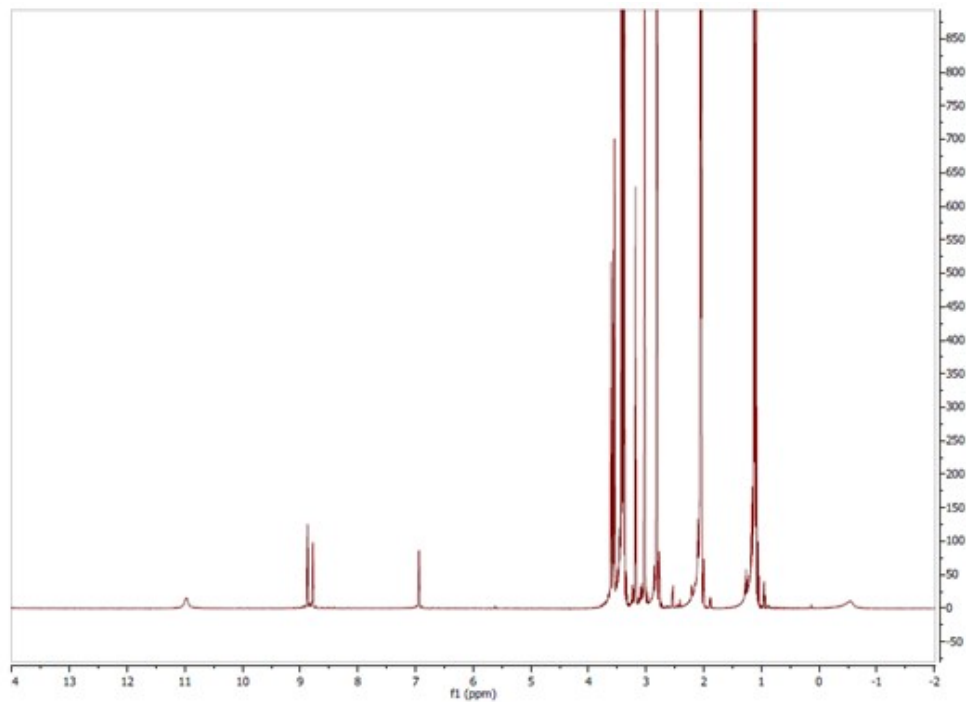


Figure S18. ^1H NMR of *fac*- $[\text{RuCl}(\text{dmsO})_3(\text{NH}=\text{C}(\text{Me})\text{pz}-\kappa^2\text{N},\text{N})](\text{OTf})$, 2a, $(\text{CD}_3)_2\text{CO}$, r. t.

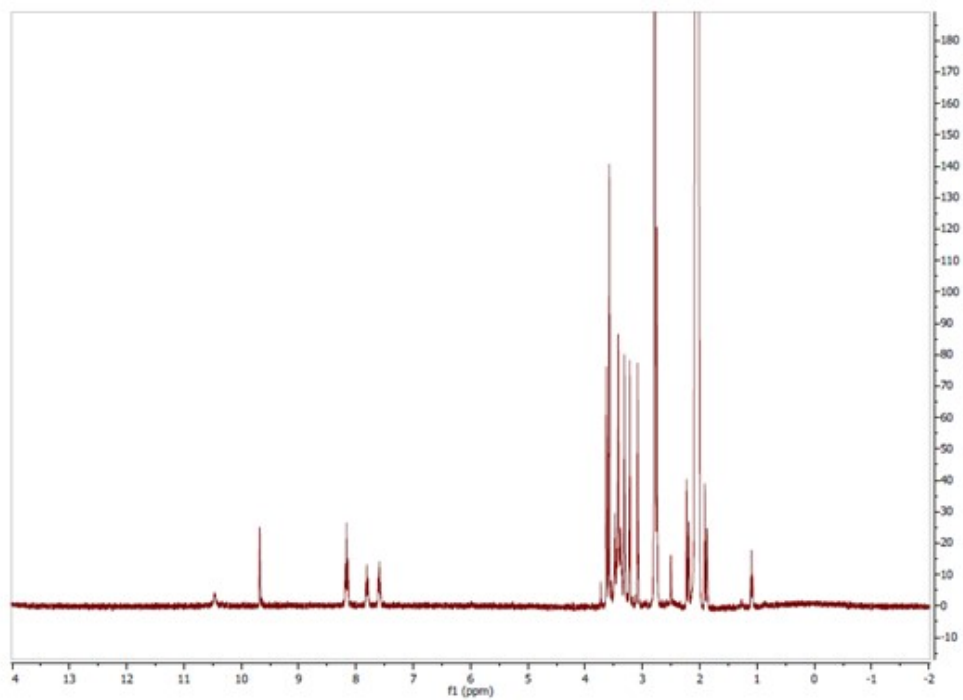


Figure S19. ^1H NMR of *fac*- $[\text{RuCl}(\text{dmsO})_3(\text{NH}=\text{C}(\text{Me})\text{indz}-\kappa^2\text{N},\text{N})](\text{OTf})$, 2b, $(\text{CD}_3)_2\text{CO}$, r. t.

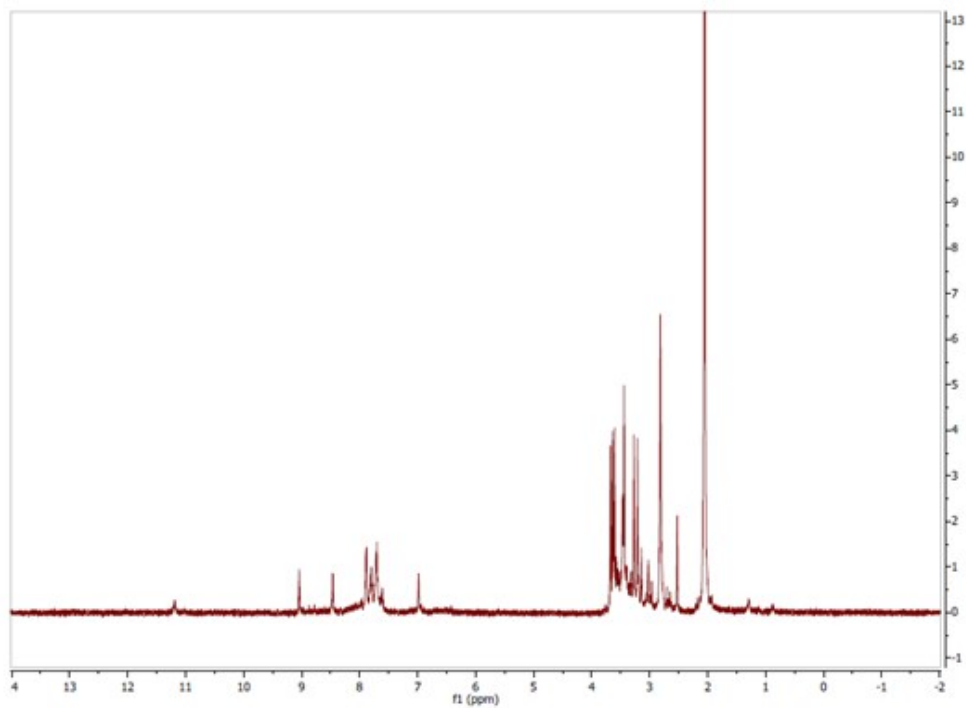


Figure S20. ¹H NMR of *fac*-[RuCl(dmsO)₃(NH=C(Ph)pz-κ²N,N)](OTf), 3a, (CD₃)₂CO, r.t.

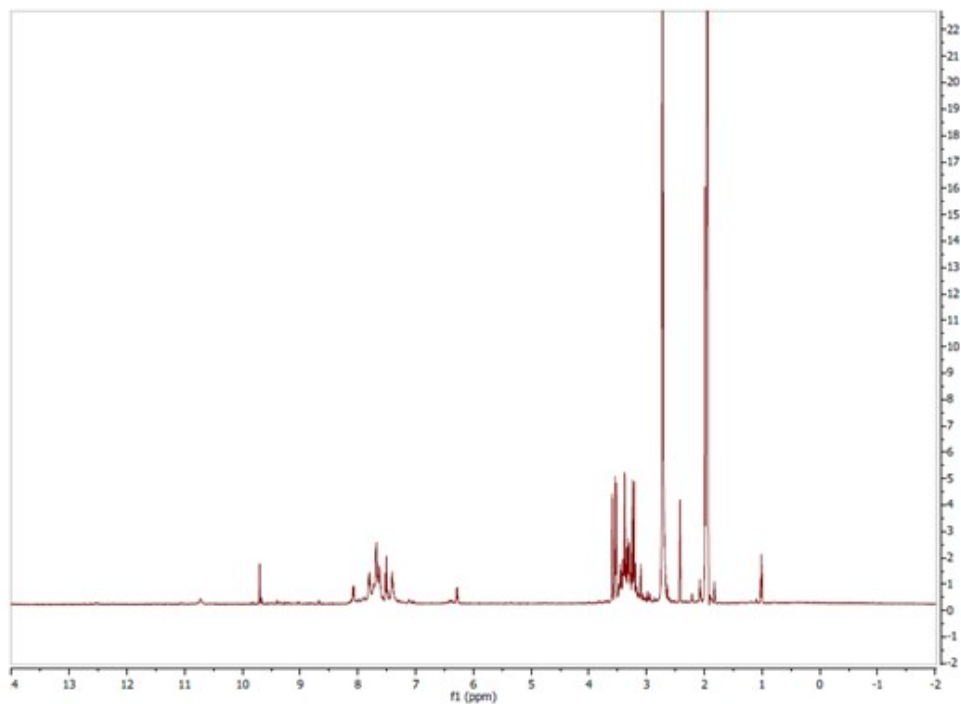


Figure S21. ¹H NMR of *fac*-[RuCl(dmsO)₃(NH=C(Ph)indz-κ²N,N)](OTf), 3b, (CD₃)₂CO, r.t.